crystals

MDPI

Article

Growth of Thin AlN Films on Si Wafers by Reactive Magnetron Sputtering: Role of Processing Pressure, Magnetron Power and Nitrogen/Argon Gas Flow Ratio

Matilde Kammer Sandager [1,2], Christian Kjelde [2] and Vladimir Popok [1,*]

[1] Department of Materials and Production, Aalborg University, 9220 Aalborg, Denmark
[2] Polyteknik AS, Moellegade 21, 9750 Oestervraa, Denmark
* Correspondence: vp@mp.aau.dk

Abstract: AlN is a wide band gap semiconductor that is of growing industrial interest due to its piezoelectric properties, high breakdown voltage and thermal conductivity. Using magnetron sputtering to grow AlN thin films allows for high deposition rates and uniform coverage of large substrates. One can also produce films at low substrate temperatures, which is required for many production processes. However, current models are inadequate in predicting the resulting structure of a thin film when different sputter parameters are varied. In this work, the growth of wurtzite AlN thin films has been carried out on Si(111) substrates using reactive direct current magnetron sputtering. The influence of the processing pressure, magnetron power and N_2/Ar ratio on the structure of the grown films has been analyzed by investigating crystallinity, residual film stress and surface morphology using X-ray diffraction, profilometry, atomic force microscopy and scanning electron microscopy. In every case, the films were found to exhibit *c*-axis orientation and tensile stress. It was found that high-quality AlN films can be achieved at an N_2/Ar ratio of 50% and a low pressure of 0.2 Pa. High magnetron powers (900–1200 W) were necessary for achieving high deposition rates, but they led to larger film stress.

Keywords: aluminum nitride; thin films; reactive magnetron sputtering; crystallinity; deposition rate; process optimization

check for updates

Citation: Sandager, M.K.; Kjelde, C.; Popok, V. Growth of Thin AlN Films on Si Wafers by Reactive Magnetron Sputtering: Role of Processing Pressure, Magnetron Power and Nitrogen/Argon Gas Flow Ratio. *Crystals* **2022**, *12*, 1379. https://doi.org/10.3390/cryst12101379

Academic Editor: Shujun Zhang

Received: 31 August 2022
Accepted: 26 September 2022
Published: 28 September 2022

Publisher's Note: MDPI stays neutral with regard to jurisdictional claims in published maps and institutional affiliations.

Copyright: © 2022 by the authors. Licensee MDPI, Basel, Switzerland. This article is an open access article distributed under the terms and conditions of the Creative Commons Attribution (CC BY) license (https://creativecommons.org/licenses/by/4.0/).

1. Introduction

AlN is a semiconductor that is of growing industrial interest due to its many potential applications in device production. With a bandgap of 6.2 eV, it can provide several orders of magnitude higher operational frequencies and withstand much higher breakdown voltages compared to Si [1]. AlN also has a very high thermal conductivity, which is crucial for heat removal in high-power devices [2]. Currently, AlN films and AlGaN heterostructures are absolutely necessary elements (buffer, transition and capping layers) of high electron mobility transistors and GaN-based diodes [3–5]. AlN thin layers are also used in the production of piezoelectric and energy harvesting devices [6,7].

The quality of the film is very important for device performance, where a high degree of *c*-axis orientation is necessary for achieving a sufficient piezoelectric response of AlN [8], while a high amount of defects or strain can generally lower functional properties [3]. The quality is highly dependent on the growth mechanics involved when making the film; however, a number of production issues are still present. In this work, reactive direct current magnetron sputtering is discussed for producing AlN thin films.

Magnetron sputtering is a good candidate for industrial success due to high deposition rates enabling fast film growth and uniform coating of large areas, the flexibility in choosing substrate material and the ability to do low-temperature growth [9]. However, reactive magnetron sputtering is a complicated process, and models that can reliably predict the resulting structure of a thin film are necessary for commercial success.

The most well-known structure zone model (SZM) for magnetron sputtered thin films was developed by Thornton in 1974 [10]. Taking inspiration from the thin film structure model proposed by Movchan and Demchishin [11], Thornton divided the film growth structures into four zones, each related to the processing pressure during film growth and homologous temperature defined by T/T_m, where T is the substrate temperature during growth and T_m is the melting temperature of the film material. In this model, the pressure defines the flux of impinging atoms, while T/T_m affects the adatom diffusion. The best crystalline quality can be reached at high temperatures, which promote mobility of deposited atoms, and relatively low pressure allowing to avoid suppression of the diffusion due to the increased flux of impinging atoms. For Zone 1, the resulting structure consists of tapered crystallites with a number of voids due to shadowing effects and low diffusion. For Zone T (transition), the film structure is determined by a mix of transport and diffusion conditions yielding films made of fiber-like grains. Zone 2 describes the formation of films consisting of wide columnar grains with faceted tops. Finally, Zone 3 yields films consisting of wide crystalline columns and/or equiaxed grains with a relatively smooth surface.

However, film growth at high substrate temperature is often not wanted in industrial processes because the difference in coefficients of thermal expansion between the film and substrate induces additional film stress when cooling to room temperature, which leads to a higher risk of the film cracking. This problem becomes even more prevalent at wafer sizes of 200 mm and larger, which are currently used in the conventional semiconductor industry. It is also found that the ratio of nitrogen flow (reactive gas) and argon flow (sputtering gas), processing pressure (i.e., pressure in the sputtering chamber during growth) as well as magnetron power are important parameters, affecting the AlN growth [12–15]. Additionally, the reactive gas can interact with the target leading to the undesirable effect of poisoning, changing the magnetron discharge conditions and causing a nonlinear behavior of deposition rate on the gas flow. This phenomenon is also known as hysteresis [16,17].

Attempts at modifying Thornton's SZM by replacing the pressure factor with a more generalized parameter, such as kinetic energy of the ions, where other effects influencing the adatom diffusion were also taken into account have been made by several groups [18,19] but the interplay between sputtering parameters was not easily encapsulated by a single variable. The presence of reactive gas further complicates this because of its significant impact on sputtering conditions caused by the hysteresis effect. Recent models also do not predict either residual film stress or deposition rates, which are of high interest to the industry.

Thus, the complex nature of interdependence of the sputtering and deposition parameters leads to a situation where the formation of high crystalline quality AlN films still requires careful consideration of growth conditions. Therefore, in the current work, the interrelation of sputtering power, operational pressure and N_2/Ar ratio are studied to optimize reactive magnetron sputtering and the formation of thin AlN films on large Si wafers and at low temperatures towards industrial applications.

2. Materials and Methods

Sample Preparation and Analysis

Prior to AlN deposition, 100 mm Si(111) wafers were soaked in acetone and cleaned in an ultrasonic bath for ten minutes, followed by rinsing with isopropanol and drying with N_2 gas.

AlN deposition is carried out using the Flextura 200 system (see Section S1 and Figure S1 in Supplementary Material for details). Al target of 3 inches in diameter with a purity of 99.999% is used for sputtering. Argon of purity 99.9999% is used as sputtering gas and molecular nitrogen of purity 99.9999% as reactive gas. All depositions are performed on 100 mm Si(111) wafers which are heated to 200 °C during film growth. The processing pressure has been varied between 0.1–1.0 Pa and magnetron power between 300–1200 W. The growth is carried out at two values of N_2/Ar gas flow ratios (determined by $\frac{N_2}{Ar+N_2} \cdot 100\%$, where N_2 and Ar are given by the flow of nitrogen and argon gas, respectively,

measured in sccm), namely 27% and 50%. Using previous experience, the growth time was adjusted for every set of used deposition parameters in order to make the films with a thickness of approximately 400 nm. The average thickness is found to be 438 ± 50 nm for the current set of samples.

Residual film stress is calculated using the modified Stoney equation [20]. Radii of curvature of wafers before and after the deposition of films are measured using XP-2 Stylus Profiler (Ambios Technology). Profiles are taken through the center of each sample both parallel and perpendicular to the wafer's flat edge with a scan length of 8 cm. The reported stress is an average of the values calculated from both profiles. Measurements are performed immediately before and after thin film deposition.

The film thickness is measured using an SE850 ellipsometer (Sentech) with an incident angle of 70°, where optical constant and film thickness are fitted according to the three-parameter Cauchy model [21]. The film thickness of every sample was found as an average of 20 measurements carried out at various locations on the surface.

X-ray diffraction (XRD) is carried out by an Empyrian (Malvern Panalytical) diffractometer with a CuKα source in Bragg–Brentano geometry. Fitting of the AlN(002) peak is performed in XPert HighScore Plus. The reported full width at half maximum (FWHM) is an average of at least 3 measurements carried out at the center, edge and intermediate position of each wafer.

Atomic force microscopy (AFM) is carried out using NTEGRA Aura (NT-MDT) system in tapping mode utilizing standard commercial cantilevers with a tip curvature radius below 10 nm. Root mean square (RMS) values of the height variations are found using Image Analysis software.

Scanning electron microscopy (SEM) images are obtained using a CrossBeam XB 1540 (Zeiss) system.

3. Results and Discussion

3.1. Influence of Magnetron Power and Processing Pressure on Deposition Rate

Having industrial applications in mind, one of the practically important factors is the deposition rate. Even if a set of growth parameters (pressure, power, gas ratio, temperature, etc.) is found to be optimal for growing films with a high crystalline quality and low surface roughness, it would be unacceptable for commercial processing if the deposition rate is low. Table 1 shows the deposition rate for samples produced at different processing pressures, magnetron powers and N_2/Ar ratios.

Table 1. Sputtering parameters and deposition rates for all produced samples.

Sample Number	Processing Pressure [Pa]	Magnetron Power [W]	N/Ar Ratio [%]	Deposition Rate [nm/min]
1	0.2	300	27	4.9
2	0.2	600	27	11.1
3	0.2	900	27	28.9
4	0.2	600	50	7.9
5	0.3	1200	50	18.1
6	0.6	600	27	8.3
7	1	600	27	7.9

Increasing the pressure in the sputtering chamber while keeping the flow ratio of N_2/Ar constant influences the deposition rate in several ways. On one hand, a higher number of Ar ions produced in the plasma and bombarding the Al target increase the sputtering rate of Al. On the other hand, an increased pressure means higher gas density causing more scattering of Al atoms on the way to the substrate. Additionally, increased partial pressure of nitrogen can lead to target poisoning, i.e., reactions of N with Al yielding AlN coating of the target which reduces the sputtering yield. Thus, the overall effect of

an increased processing pressure is some decrease in the deposition rate as can be seen in Table 1 for a constant magnetron power of 600 W.

Meanwhile, an increase in the magnetron power has a much more significant effect. It can be seen in Table 1 that at a constant pressure of 0.2 Pa, the deposition rate is significantly increased reaching 28.9 nm/min at 900 W. However, the growth of stoichiometric AlN requires a sufficient supply of nitrogen. Therefore, an increase in power providing high concentrations of Al should be supplemented by increasing the flow of N_2. Yet, this also leads to a higher level of target poisoning, which reduces the sputtering yield, and thus the deposition rate. This tendency is evident in the case where the power is 1200 W and the N_2/Ar ratio is 50%. Despite the higher power, the deposition rate is significantly lower (18.1 nm/min) compared to the case where the power is 900 W and the N_2/Ar ratio is 27% (28.9 nm/min). However, some level of target poisoning might be unavoidable for correct stoichiometry to be achieved [22]. Now, considering the sputtering parameters for acceptable deposition rates one should have a look into the film quality.

3.2. Film Stress, XRD Analysis and Surface Morphology of AlN Thin Films

3.2.1. Effect of Changing the Processing Pressure and N_2/Ar Ratio

Figure 1 shows the XRD spectra of the produced films. The prominent peak around 36° belonging to AlN(002) indicates an oriented growth along the *c*-axis of wurtzite-type hexagonal structure in all cases [23]. The small peak at 76° can be assigned to AlN(004) further supporting the preferential *c*-axis orientation of the films. The reflection at approximately 59° originates from the Si(111) substrate. Since the AlN(002) peak is the most prominent peak for all films, as seen in Figure 1, the FWHM values of these peaks are further analyzed together with the calculated film stress for different growth parameters. It is worth mentioning that FWHM values can be used for estimation of film quality; low FWHM is typically assigned to good crystalline quality [24,25].

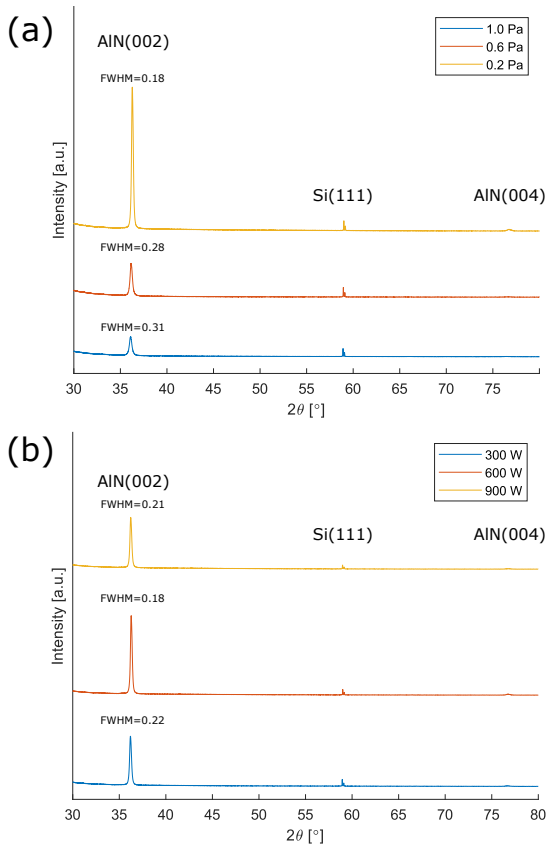


Figure 1. *Cont.*

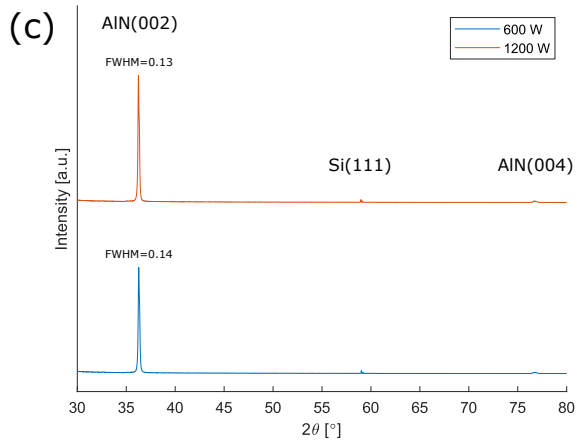


Figure 1. XRD spectra of AlN films grown on Si(111) where (**a**) processing pressure is varied while magnetron power is kept constant at 600 W and N_2/Ar ratio at 27%, (**b**) magnetron power is varied while processing pressure is kept constant at 0.2 Pa and N_2/Ar ratio at 27%, and (**c**) magnetron power is varied while processing pressure is kept constant at 0.2 Pa and N_2/Ar ratio at 50%. FWHM of the AlN(002) peak is indicated for each spectrum.

Figure 2 shows the calculated film stress and FWHM of the AlN(002) peak for three samples grown at 0.2 Pa, 0.6 Pa and 1.0 Pa. Magnetron power of 600 W and N_2/Ar ratio of 27% are kept constant for these samples.

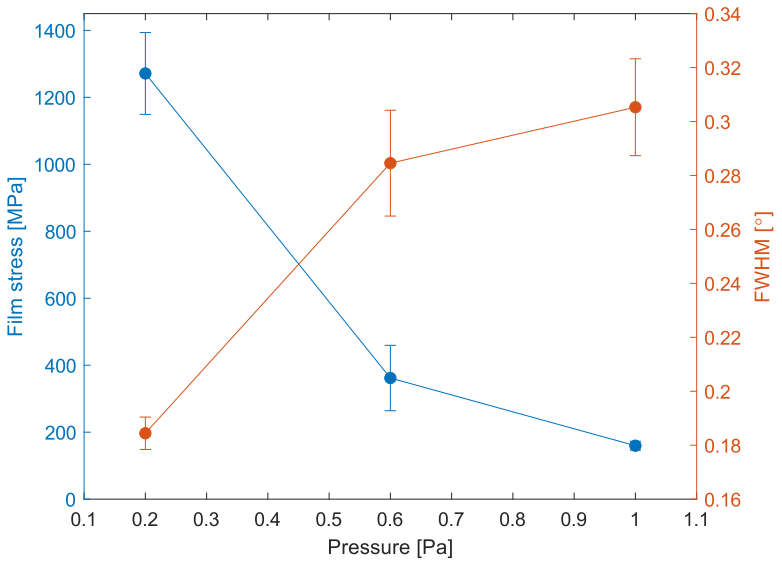


Figure 2. Film stress and FWHM of the AlN(002) peak for films grown using different processing pressures.

When the processing pressure is increased, the mean free path of sputtered atoms on the way to the substrate is decreased, and energy lost in collisions reduces the mobility of adatoms on the substrate surface. A higher number of collisions also increases the likelihood of Al atoms arriving at oblique angles to the substrate, thus, enhancing the effects of shadowing [26]. These considerations bring us to the expectation that an increase in processing pressure while keeping other parameters constant would lead to Zone 1 conditions in the SZM. Indeed, the FWHM is found to increase significantly with pressure indicating that the best crystalline quality and level of *c*-axis orientation is obtained at the lowest pressure of 0.2 Pa. This case corresponds to the highest tensile stress due to a large lattice mismatch between AlN and Si [27]. Deposition at increased pressure causes a less perfect crystalline structure with defects providing release of the stress.

In Figure 3 cross-sectional SEM images of two selected samples can be seen.

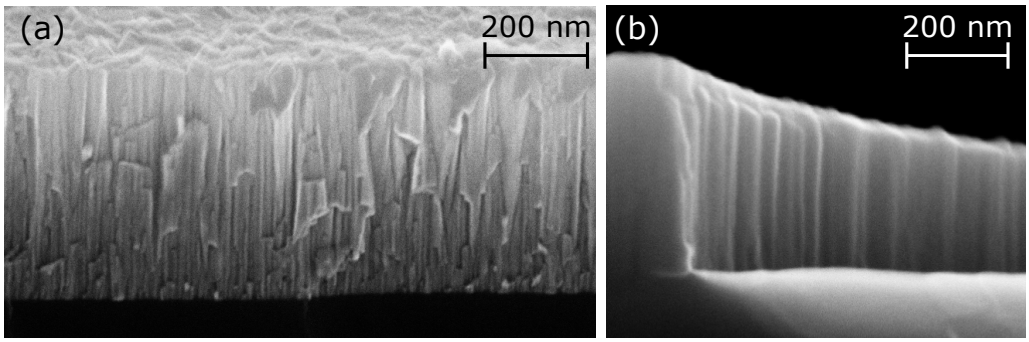


Figure 3. Cross-sectional SEM images of samples produced using an N_2/Ar ratio of (**a**) 27% and (**b**) 50%. A magnetron power of 600 W and a processing pressure of 0.2 Pa are kept constant.

In Figure 3a one can see that the film consists of tapered columnar structures, which are narrow at the interface with Si and grow wider at the top. This type of structure is consistent with Zone 1 of Thornton's SZM. When the N_2/Ar ratio is increased to 50%, the film is found to be denser, and columns appear to be wider extending through the entire film as seen in Figure 3b. These are characteristics typically associated with Zone T and Zone 2 in Thornton's SZM. Thus, increasing the N_2/Ar gas ratio leads to structural changes similar to those typical for higher temperatures despite the fact that the actual growth temperature was kept low at 200 °C. This is an important finding for the optimization towards commercial processing.

In Figure 4, SEM and AFM images of three selected samples are shown.

The surface of the sample deposited at 0.2 Pa consists of small round grains and a number of larger elongated plate-like inclusions, as seen in Figure 4a,d. The small grains are the tops of the columnar structures shown in Figure 3. The larger inclusions are believed to be abnormally oriented grains (AOGs) exhibiting a different crystal orientation than the rest of the film. They are likely to form at grain boundaries [28] and have been found to be correlated to deposition processes where off-sputtered atoms have a short mean free path, which can cause AlN cluster formation in the gas mixture before arriving at the substrate surface [29,30]. AOGs are generally problematic because higher surface roughness and lower degree of (0001)-orientation reduces the piezoelectric response and thus inhibit device performance [29]. The film grown at 1.0 Pa has a rougher surface (see Figure 4b,e) compared to that of the case of 0.2 Pa, which can be explained by the reduced adatom mobility on the substrate. One can also see a higher contribution of AOGs.

Increasing the N_2/Ar ratio to 50% causes a significant reduction in the AOGs density resulting in a smooth surface topography with an RMS value of only 0.9 nm (see Figure 4c,f). This agrees with the XRD measurements for this sample, where the FWHM of the (002)-peak was found to be only 0.14° (see Figure 1c) indicating better crystalline quality. However, the drawback of this good quality film is a lower deposition rate (see Table 1) and moderately high stress, which was found to be 885 MPa.

3.2.2. Effect of Changing the Magnetron Power

Figure 5 shows the calculated film stress and FWHM of the AlN(002) peak for three samples grown at 300 W, 600 W and 900 W. Processing pressure of 0.2 Pa and an N_2/Ar ratio of 27% are kept constant.

When the power is increased from 300 W to 600 W, the FWHM decreases considerably. This tendency can be explained in the following way: when magnetron power is increased, the flux of arriving Al atoms increases as well as the kinetic energy with which they bombard the substrate. These collisions can cause heating of the substrate [31] leading to increased adatom diffusion corresponding to Zone T conditions. While the increased substrate temperature (due to the collisions of energetic particles with the surface) can

lead to better crystalline quality, the film stress is increased as can be seen in Figure 5. The influence on the FWHM and film stress when the power is increased from 600 to 900 W is less clear. It could be an interrelation between the above-mentioned collision-induced additional heating and a higher flux of sputtered Al. However, this case requires further study.

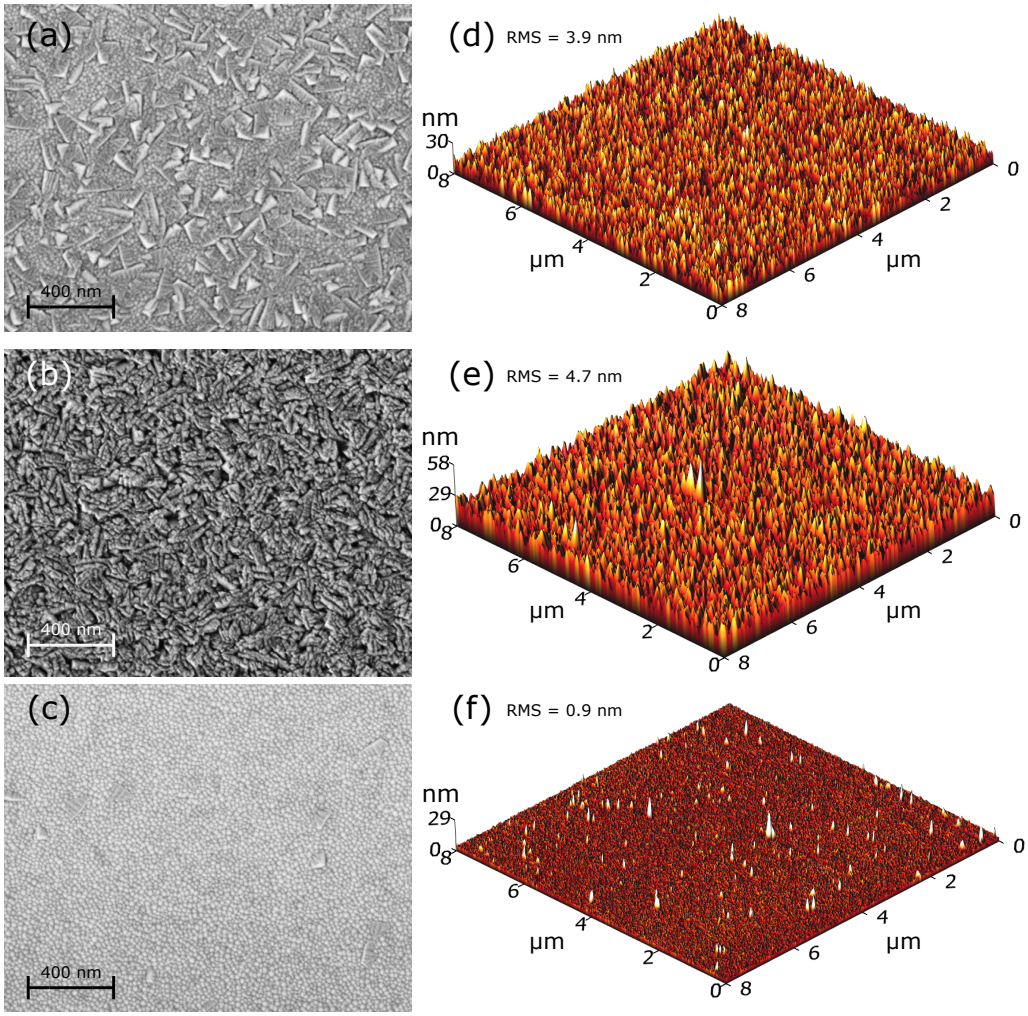


Figure 4. (**Left** column) SEM and (**right** column) AFM images of the samples produced at (**a**,**d**) a pressure of 0.2 Pa and an N_2/Ar ratio of 27%, (**b**,**e**) pressure of 1.0 Pa and N_2/Ar ratio of 27% and (**c**,**f**) pressure of 0.2 Pa and N_2/Ar ratio of 50%. Magnetron power is kept constant at 600 W. RMS values are given in correspondence to every AFM image.

In Figure 6, SEM and AFM images of two selected samples produced at different magnetron power can be seen.

The SEM images in Figure 6a,b show a similar surface morphology with a high density of AOGs present at both powers. In Figure 6c,d, it can be seen that the surface roughness is slightly lower at 900 W (3.4 nm) compared to that of 300 W (5.8 nm), likely caused by the increased adatom diffusion due to the higher energy of incoming Al particles as well as the collision-induced temperature increase discussed above. The observation that increasing the magnetron power does not seem to worsen film quality nor cause roughening of the film surface is of interest because it allows for achieving good quality film at high deposition rates, however, at the expense of high film stress as can be seen in Figure 5.

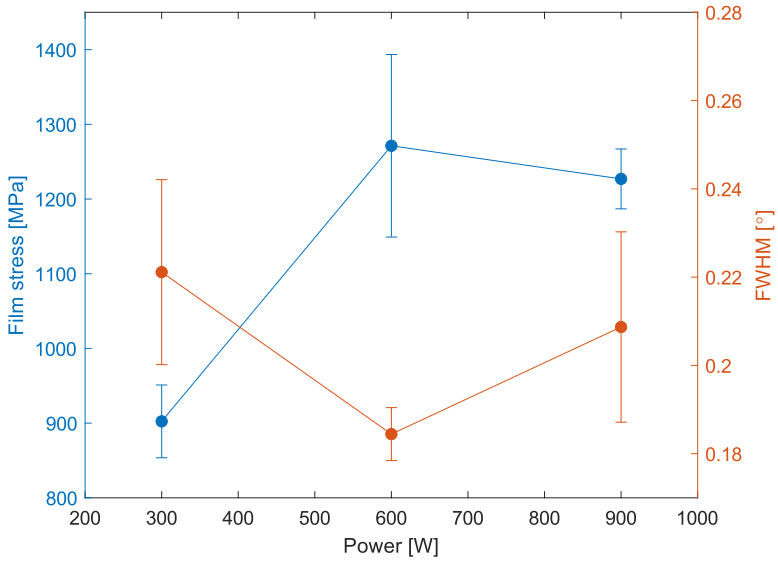


Figure 5. Film stress and FWHM of the AlN(002) peak for films grown using different powers.

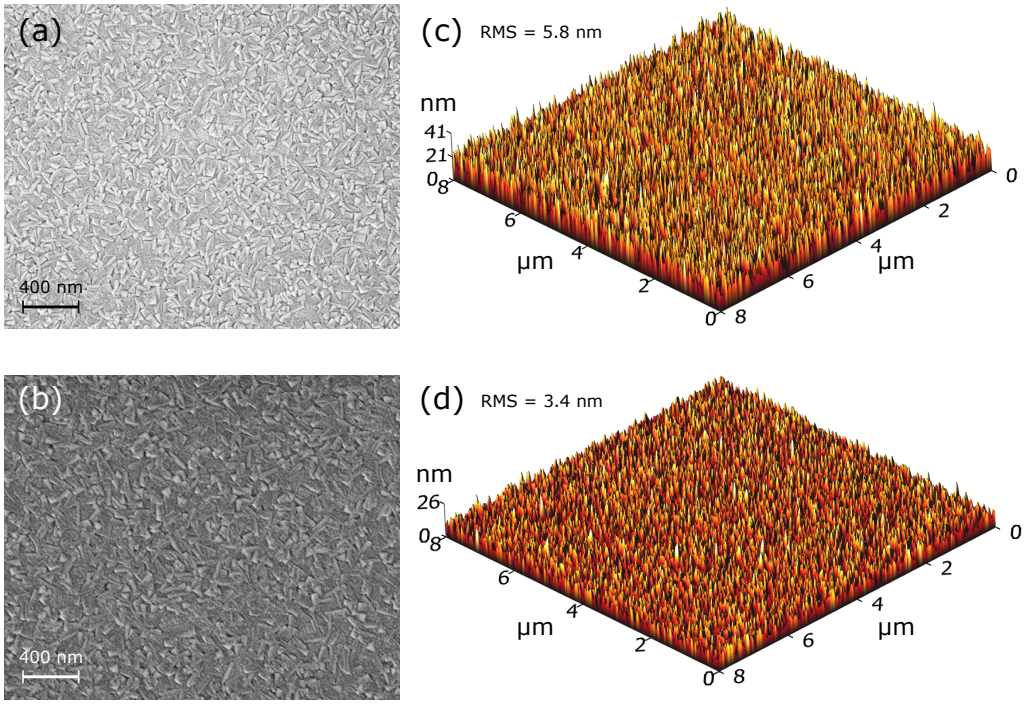


Figure 6. (**Left** column) SEM and (**right** column) AFM images of the the samples produced at a magnetron power of (**a**,**c**) 300 W and (**b**,**d**) 900 W. A processing pressure of 0.2 Pa and an N_2/Ar ratio of 27% is kept constant. RMS values are given in correspondence to every AFM image.

4. Conclusions

The growth of AlN thin films is a complex process and SZM based primarily on changes in homologous temperature and processing pressure is insufficient for predicting the final film structure. It is shown in this work that magnetron power is an important parameter allowing to increase the deposition rate. At the same time, the magnetron power also affects the kinetic energy of the impinging atoms and, thus, can act to some extent as a temperature factor; increased power leads to higher kinetic energy which facilitates surface diffusion of adatoms (similar to increased substrate temperature) and growth of films with better crystalline quality and lower surface roughness. For reactive magnetron sputtering,

the ratio of reactive and processing gases (N_2 to Ar in this case) is another important parameter affecting the crystallinity, on one hand, but also influencing the deposition rate, on the other hand.

It is hardly possible to provide growth conditions that allow for simultaneously achieving high crystalline quality, low surface roughness, low residual stress and high deposition rate. However, it is possible to reach some compromises and they are suggested in the tendency diagram illustrated in Figure 7, which is based on the results of the current work. The use of a high N_2/Ar gas flow ratio while keeping the processing pressure low provides the best way to grow films with good crystalline quality and low surface roughness. However, these conditions promote target poisoning and reduce the deposition rate, which is an industrially important factor. Tuning the magnetron power can help to strike the desired balance between residual stress and deposition rate. On the other hand, the studies focused on growth utilizing a low N_2/Ar ratio of 27% allow us to conclude that films of not superior but acceptable quality (in terms of crystallinity and surface roughness) can be obtained while prioritizing a high deposition rate.

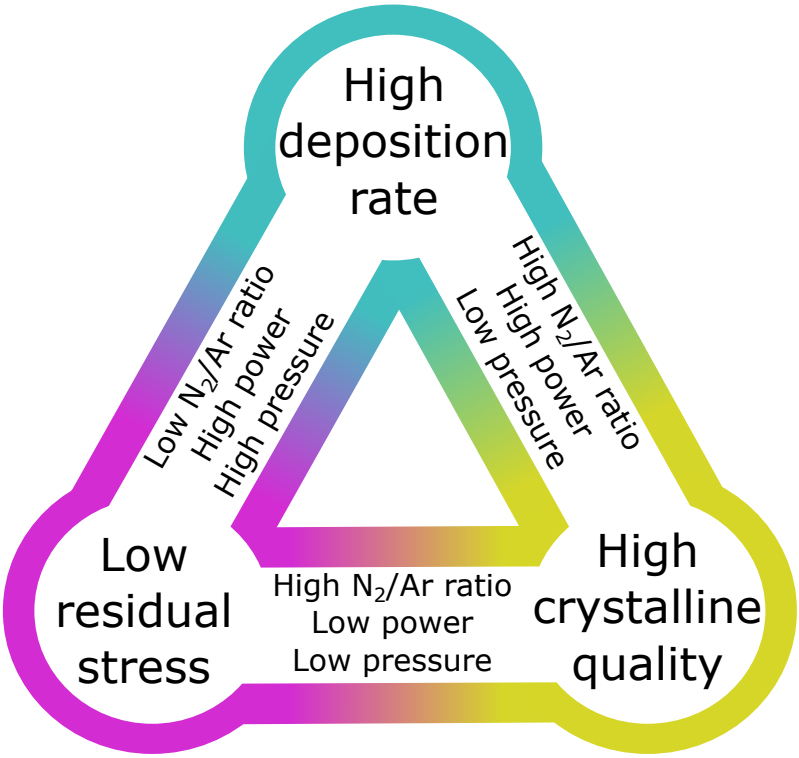


Figure 7. Diagram showing how residual stress, crystalline quality and deposition rate are related to sputtering parameters.

Supplementary Materials: The following supporting information can be downloaded at: https://www.mdpi.com/article/10.3390/cryst12101379/s1, Section S1: Sputtering Apparatus; Figure S1: Schematic illustration of the main chambers and parts of Flextura 200.

Author Contributions: Conceptualization, C.K. and V.P.; methodology, M.K.S. and V.P.; formal analysis, M.K.S.; investigation, M.K.S.; writing—original draft preparation, M.K.S.; writing—review and editing, C.K. and V.P.; visualization, M.K.S.; supervision, C.K. and V.P. All authors have read and agreed to the published version of the manuscript.

Funding: This research was funded by Innovation Fund Denmark within Industrial PhD project on Tailoring the Metal-Nitride Films for Power Electronics (TAMPE).

Data Availability Statement: Not applicable.

Conflicts of Interest: The authors declare no conflict of interest.

References

1. Tsao, J.Y.; Chowdhury, S.; Hollis, M.A.; Jena, D.; Johnson, N.M.; Jones, K.A.; Kaplar, R.J.; Rajan, S.; Van de Walle, C.G.; Bellotti, E.; et al. Ultrawide-bandgap semiconductors: Research opportunities and challenges. *Adv. Electron. Mat.* **2018**, *4*, 1600501. [CrossRef]
2. Hickman, A.L.; Chaudhuri, R.; Bader, S.J.; Nomoto, K.; Li, L.; Hwang, J.C.M.; Xing, H.G.; Jena, D. Next generation electronics on the ultrawide-bandgap aluminum nitride platform. *Semicond. Sci. Technol.* **2021**, *36*, 044001. [CrossRef]
3. Amano, H.; Baines, Y.; Beam, E.; Borga, M.; Bouchet, T.; Chalker, P.R.; Charles, M.; Chen, K.J.; Chowdhury, N.; Chu, R.; et al. The 2018 GaN power electronics roadmap. *J. Phys. D Appl. Phys.* **2018**, *51*, 163001. [CrossRef]
4. Kim, N.;Yu, J.; Zhang, W.; Li, R.; Wang, M.; Ng, W.T. Current trends in the development of normally-OFF GaN-on-Si power transistors and power modules: A review. *J. Electron. Mater.* **2020**, *49*, 6829–6843. [CrossRef]
5. Popok, V.; Aunsborg, T.S.; Godiksen, R.H.; Kristensen, P.K.; Juluri, R.R.; Caban, P.; Pedersen, K. Structural characterization of the MOVPE grown AlGaN/GaN for HEMT formation. *Rev. Adv. Mater. Sci.* **2018**, *57*, 72–81. [CrossRef]
6. Iqbal, A.; Mohd-Yasin, F. Reactive sputtering of aluminum nitride (002) thin films for piezoelectric applications: A review. *Sensors* **2018**, *18*, 1797. [CrossRef]
7. Fei, C.; Liu, X.; Zhu, B.; Li, D.; Yang, X.; Yang, Y.; Zhou, Q. AlN piezoelectric thin films for energy harvesting and acoustic devices. *Nano Energy* **2018**, *51*, 146–161. [CrossRef]
8. Tonisch, K.; Cimalla, V.; Foerster, C.; Romanus, H.; Ambacher, O.; Dontsov, D. Piezoelectric properties of polycrystalline AlN thin films for MEMS application. *Sens. Actuators A* **2006**, *132*, 658–663 [CrossRef]
9. Prabaswara, A.; Birch, J.; Junaid, M.; Serban, E.A.; Hultman, L.; Hsiao, C.L. Review of GaN thin film and nanorod growth using magnetron sputter epitaxy. *Appl. Sci.* **2020**, *10*, 3050. [CrossRef]
10. Thornton, J.A. Structure and topography of sputtered coatings. *J. Vac. Sci. Technol.* **1974**, *11*, 666. [CrossRef]
11. Movchan, B.A.; Demichishin, A.V. Structure and properties of thick condensates of nickel, titanium, tungsten, aluminum oxides, and zirconium dioxide in vacuum. *Fiz. Met. Metalloved.* **1969**, *28*, 653.
12. Kar, J.P.; Bose, G.; Tuli, S. Influence of nitrogen concentration on grain growth, structural and electrical properties of sputtered aluminum nitride films. *Scr. Mater.* **2006**, *54*, 1755–1759. [CrossRef]
13. Kusaka, K.; Taniguchi, D.; Hanabusa, T.; Tominaga, K. Effect of input power on crystal orientation and residual stress in AlN deposited by dc sputtering. *Vacuum* **2000**, *59*, 806–813. [CrossRef]
14. Iriarte, G.F.; Rodriguez, J.G.; Calle, F. Effect of substrate-target distance and sputtering pressure in the synthesis of AlN thin films. *Microsyst. Technol.* **2011**, *17*, 381–386. [CrossRef]
15. Lan, Y.; Shi, Y. Effect of working pressure and annealing temperature on single-phase AlN films. *Mater. Lett.* **2018**, *213*, 1–3. [CrossRef]
16. Strijckmans, K.; Schelfhout, R.; Depla, D. Tutorial: Hysteresis during the reactive magnetron sputtering process. *J. Appl. Phys.* **2018**, *124*, 241101. [CrossRef]
17. Berg, S.; Blom, H.-O.; Larsson, T.; Nender, C. Modeling of reactive sputtering of compound materials. *J. Vac. Sci. Technol. A* **1986**, *5*, 202. [CrossRef]
18. Messier, R.; Giri, A.P.; Roy, R.A. Revised structure zone model for thin film physical structure. *J. Vac. Sci. Technol. A* **1984**, *2*, 500. [CrossRef]
19. Anders, A. A structure zone diagram including plasma-based deposition and ion etching. *Thin Solid Films* **2010**, *508*, 4087–4090. [CrossRef]
20. Flinn, P.A.; Gardner, D.S.; Nix, W.D. Measurement and interpretation of stress in aluminum-based metallization as a function of thermal history. *IEEE Trans. Electron. Devices* **1987**, *ED-34*, 689–699.
21. Shah, D.; Patel, D.; Hilfiker, J.; Linford, M. A tutorial on spectroscopic ellipsometry (SE), 2. The Cauchy model. *Vac. Technol. Coat.* **2019**, *May*, 1–5.
22. Berg, S.; Nyberg, T. Fundamental understanding and modeling of reactive sputtering processes. *Thin Solid Films* **2005**, *476*, 215–230. [CrossRef]
23. Jiao, X.; Shi, Y.; Zhong, H.; Zhang, R.; Yang, J. AlN thin films deposited on different Si-based substrates through RF magnetron sputtering. *J. Mater. Sci. Mater. Electron.* **2015**, *26*, 801–808. [CrossRef]
24. Hordon, M.J.; Averbach, B.L. X-ray measurements of dislocation density in deformed copper and aluminum single crystals. *Acta Metall.* **1961**, *9*, 237–246. [CrossRef]
25. Heinke, H.; Kirchner, S.; Einfeldt, S.; Hommel, D. X-ray diffraction analysis of the defect structure in epitaxial GaN. *Appl. Phys. Lett.* **2000**, *77*, 2145. [CrossRef]
26. Flickyngerová, S. Effects of sputtering power and pressure on properties of ZnO:Ga thin films prepared by oblique-angle deposition. *Thin Solid Films* **2011**, *520*, 1233–1237. [CrossRef]
27. Kukushkin, S.A.; Osipov, A.V.; Bessolov, V.N.; Medvedev, B.K.; Nevolin, V.K.; Tcarik, K.A. Substrates for epitaxy of gallium nitride: New materials and techniques. *Rev. Adv. Mater. Sci.* **2008**, *17*, 1–32.
28. Sandu, C.S.; Parsapour, F.; Mertin, S.; Pashchenko, V.; Matloub, R.; LaGrange, T.; Heinz, B.; Muralt, P. Abnormal grain growth in AlScN thin films induced by complexion formation at crystallite interfaces. *Phys. Status Solidi A* **2019**, *216*, 1800569. [CrossRef]

29. Lu, Y.; Reusch, M.; Kurz, N.; Ding, A.; Christoph, T.; Kirste, L.; Lebedev, V.; Žukauskaitė, A. Surface morphology and microstructure of pulsed DC magnetron sputtered piezoelectric AlN and AlScN thin films. *Phys. Status Solidi A* **2018**, *215*, 1700559. [CrossRef]
30. Reusch, M. Analysis and optimization of sputter deposited AlN-layers for flexural plate wave devices. *J. Vac. Sci. Technol. B* **2016**, *34*, 052001. [CrossRef]
31. Krishnasamy, J.; Chan, K.-Y.; Tou, T.-Y. Influence of process parameters on the substrate heating in direct current plasma magnetron sputtering deposition process. *Microelectron. Int.* **2010**, *27*, 75–78. [CrossRef]